

STRUCTURE AND PROPERTIES OF HIGH-FIELD SUPERCONDUCTORS

J.D. Livingston
General Electric Company
Research and Development Center
Schenectady, New York

I. INTRODUCTION

The intent of this paper is to review recent literature on the relation between structure and properties in high-field superconductors. Critical temperatures and fields will be discussed briefly, but emphasis will be on critical currents and flux pinning, where metallurgical microstructure plays its major role. For a comprehensive review of earlier structure-properties studies in superconductivity, see Livingston and Schadler.¹

II. CRITICAL TEMPERATURES AND FIELDS

High-Field Materials

Most elemental superconductors are type I superconductors with maximum critical fields below 1000 Oe. Most alloy and compound superconductors are type II superconductors, but only a limited number have very high critical fields. If we arbitrarily define "high-field" superconductors as those having critical fields greater than 50 kOe, high-field materials known today fall into three structural classes:

1) Body-centered-cubic alloys, such as NbZr and NbTi. Most superconducting magnets have been, and are being, made with these materials. NbTi appears to be superseding NbZr because of higher critical fields and easier fabrication.

2) Interstitial compounds with the NaCl (B1) crystal structure, such as NbN. Difficulties in producing and handling these compounds have so far precluded any commercial application. However, the recent observation of high critical currents obtained by a thin-film sputtering technique² is promising.

3) Compounds of the "β-tungsten" (A15) structure, such as Nb₃Sn and V₃Ga. Superconducting magnets producing fields of 100 kOe and higher are already being produced with several varieties of commercially-available Nb₃Sn.

Critical Temperatures

High values of the critical temperature, T_c , are of interest not only in themselves, but also because they directly influence the thermodynamic critical field $H_c(T)$, which is proportional to $T_c[1 - (T/T_c)^2]$, and which in turn limits our ultimate critical currents.

Critical temperatures of superconducting materials have been tabulated by Roberts.³ For bcc alloys, the highest known T_c is near 14°K, but the commercially-available alloys are generally in the range of 9-11°K. Extensive study of the interstitial compounds⁴ has revealed compositions in the NbCN and NbTiN systems with critical temperatures near 18°K.

Several A15 compounds, including Nb₃Sn, have critical temperatures near 18°K.⁵ A ternary compound of approximate composition Nb₃Al_{0.8}Ge_{0.2} was reported last year⁵

to have a critical temperature of 20°K. More recent work, in which composition and order in this ternary system were believed to be optimized, has produced a critical temperature of 20.7°K.⁶ This T_c , slightly above the boiling point of liquid hydrogen (at a pressure of one atmosphere), is the highest known critical temperature.

Our fundamental understanding of what determines T_c in a particular superconductor is very limited. The BCS theory indicates that T_c increases very sensitively with the product NV , where N is the density of states at the Fermi surface, and V is the electron-electron interaction parameter. However, the high- T_c materials have complex band structures, and even their normal-state properties are not well understood. The parameter N is, in principle, obtainable from the zero-temperature limit of the normal-state specific heat. (Experimental limitations, however, require considerable extrapolation in high-field materials.) The parameter V remains essentially underivable from first principles, and thus is generally inferred from T_c , rather than vice versa.

Broadly, it appears that the β -tungsten compounds with high T_c have a high N (and low V), while the high- T_c interstitial compounds have a low N (and high V).⁷ Much more theoretical and experimental work is necessary to improve our understanding of the electron structure of these materials. From the viewpoint of metallurgical structure, the major need is more information on the effect of stoichiometry, alloying, and order on T_c . The relation between the cubic-tetragonal martensitic transformation observed in some of these materials and their superconducting critical temperature also remains obscure.⁸

Critical Fields

The major basis for our understanding of the critical fields of type II superconductors is the GLAG (Ginzburg-Landau-Abrikosov-Gorkov) theory. According to this theory, the bulk upper critical field is given by $H_{c2} = \sqrt{2\kappa}H_c$. The dimensionless Ginzburg-Landau parameter κ can be written approximately as $\kappa_\ell + \kappa_0$, where the "extrinsic" part, κ_ℓ , is proportional to $N^2\ell^{-1}$ (ℓ is the electron mean free path), and the "intrinsic" part, κ_0 , is proportional to $T_c N^{3/2}$, and independent of ℓ . In many high-field superconductors, the upper critical field does not fully reach the GLAG H_{c2} because of paramagnetic effects. The various factors affecting critical fields are reviewed in depth by Cody.⁹

For bcc alloys¹⁰ and the interstitial compounds,^{11,12} the maximum upper critical fields appear to be roughly 150 kOe. In these materials, $\kappa_\ell \gg \kappa_0$,¹³ and they may be called "extrinsic" high-field superconductors. Several β -tungsten compounds, in particular Nb₃Sn, have critical fields approaching 250 kOe. Because of their high N , these materials appear to have $\kappa_0 \gg \kappa_\ell$, and are believed to be "intrinsic" high-field superconductors.^{14,15} Hake¹⁶ has recently suggested that their critical fields could perhaps be increased even further if they could be produced with shorter mean free paths, i.e., with both κ_0 and κ_ℓ large. He suggested an ultimate upper limit for Nb₃Sn of about 830 kOe.

Recent preliminary measurements using pulsed fields show that a NbAlGe compound, prepared after the prescription described by Matthias et al.,⁵ was still superconducting at 4.2°K and 265 kOe.¹⁷ It is interesting that this material has a higher critical field than Nb₃Sn despite a significantly smaller N , which implies a smaller κ_0 . It is possible that ternary alloying has produced a shorter mean free path and increased κ_ℓ .

More work is needed to clarify the effect of mean free path on upper critical field in the β -tungsten compounds. The major effect of metallurgical structure on critical fields is through the effect of defects on ℓ , and, hence, on κ_ℓ . It perhaps should also be mentioned that, at surfaces between superconductors and nonconducting phases, a superconducting "sheath" can persist to $H_{c3} \approx 1.7 H_{c2}$. It is possible that the effective critical field of some superconductors could be increased by producing a large amount

of such internal surfaces, perhaps with oxide inclusions, for example. Critical fields for nucleation of superconductivity at internal surfaces have recently been considered theoretically by Boyd¹⁸ and Tilley.¹⁹

III. CRITICAL CURRENTS

Critical currents in the mixed state (between H_{C1} and H_{C2}) are controlled by the interaction between the metallurgical and magnetic microstructures. As in the analogous fields of mechanical and ferromagnetic properties, commercially interesting "hard" properties result not from homogeneous, well-annealed specimens, but from internally heterogeneous microstructures. To see why, we first consider a relatively homogeneous type II superconductor.

The Flux Lattice

Until very recently, the magnetic microstructure of the mixed state was known only from theory and from indirect experiments such as neutron diffraction²⁰ and nuclear magnetic resonance.²¹ However, in a beautiful series of experiments, Trüble and Essmann²²⁻²⁵ have succeeded in directly observing the flux lattice of the mixed state (Fig. 1). As predicted by theory, a hexagonal lattice of flux threads containing one flux quantum ($\Phi_0 = 2 \times 10^{-7}$ G·cm²) each is observed. The lattice, however, is found to be highly imperfect, the major defects observed being "dislocations" in the flux lattice (Fig. 2).^{24,26}

The equilibrium flux lattice spacing, and, hence, the internal flux density B , is determined by a balance between the magnetic pressure of the externally applied field and the mutual repulsive forces between flux threads. The repulsive force between flux threads increases rapidly as the interthread spacing d decreases, eventually varying as $1/d$ at small d . In a homogeneous sample, these interthread forces lead to a uniform B throughout the sample (except in the immediate vicinity of the surface).

If one attempts to impose a bulk current of density J transverse to the flux threads, the threads experience a force transverse to both B and J , commonly called a Lorentz force. From the flux lattice point of view, this force can be looked upon as resulting from the gradient in B that is necessitated by J through Maxwell's equations. (A flux thread in a flux gradient, of course, experiences more repulsive interthread forces from one side than the other, yielding a net force directed down the flux gradient.) In a homogeneous specimen, flux threads will move in response to this force, producing losses and therefore electrical resistance. Thus a homogeneous specimen can carry no lossless bulk current in the mixed state.

In an inhomogeneous sample, however, variations in flux thread line energy from point to point can yield "pinning forces" that can resist the "Lorentz forces" resulting from flux gradients. Thus internal flux gradients, i.e., bulk currents, can occur, and can be observed (Fig. 3). It is found that the gradient in lattice parameter (gradient in B) can be related through standard lattice theory to the net density of flux lattice dislocations of one sign.²⁵

When the surface fields of a sample in the mixed state are change by changing applied currents or fields, flux threads will move in response only as long as the resulting flux gradient forces (Lorentz forces) are greater than the local pinning forces. Thus, when static conditions are reached, the two forces will be locally in balance. The flux gradient force in dyn/cm³ is given approximately by $JB/10$, if J is in A/cm², and B is in gauss. The static flux distribution expected, therefore, in an inhomogeneous type II superconductor in the mixed state, will everywhere exhibit a critical current density $J_c = 10 F_p/B$, where F_p is the net pinning force per unit volume. If we consider instead the net pinning force f_p per flux thread per unit length, we get

$J_c = 10 f_p / \phi_0$, since each flux thread contains one flux quantum ϕ_0 . Thus $J_c = 5 \times 10^7 f_p$, where f_p is in dyn/cm. We defer the question of the B dependence of f_p (or F_p) to a later section.

The Critical State (Bean Model)

We have seen that the balance between pinning forces and "Lorentz" forces (actually a flux-gradient force produced by interthread repulsive forces) yields a bulk critical current density J_c . The existence of this parameter J_c is the basis of the critical state model for high-field superconductors, first introduced by Bean,²⁷ independently conceived by London,²⁸ and subsequently developed by Anderson and Kim.²⁹⁻³¹

The detailed verification of this model has been extensive in recent years. The theory is supported, for example, by quantitative relations between magnetization curves and transport current data,^{32,33} by the influence of transport current on magnetization,^{34-36,*} by specimen-size-dependent effects,^{27,38-40} and by detailed experiments with alternating fields and currents.⁴¹⁻⁴⁴ Perhaps the most dramatic experiments, however, are those which directly probe the macroscopic flux distribution within inhomogeneous high field superconductors in the mixed state.^{45,46} For example, the results in Fig. 4 are much like the schematic diagrams of flux penetration appearing in Bean's early papers.

The data in Fig. 4 demonstrate two other significant points. First, it is clear that the critical internal flux gradient, and, therefore, J_c , decreases with increasing B. Although Bean's first paper assumed J_c constant for mathematical simplicity, the B-dependence of J_c was recognized by him and is generally accounted for by workers using the critical state model. Some of the forms for the B-dependence of J_c appearing in the literature are B^{-1} (which results if F_p is constant),^{29,47,48} $B^{-\frac{1}{2}}$,³⁶ $B^{-\gamma}$,⁴⁹ $(B+B_0)^{-1}$,^{30,31} $(H_{c2}-B)$,⁵⁰ and $B^{-\frac{1}{2}}(H_{c2}-B)$.^{33,51,52} No single form for $J_c(B)$ applies generally all the way from H_{c1} to H_{c2} . This complicates, but in no way invalidates, application of the critical state model.

Another feature of Fig. 4, however, shows a serious limitation of the application of the simple critical state model to real materials. At five different occasions as the field was increased, magnetic flux abruptly penetrated the specimen completely, as if the specimen had temporarily lost all flux-shielding capability. These flux jumps result from a thermal instability that cannot be treated by the simple isothermal Bean model. Extensions of the Bean model to include the heating produced by flux motion have been made, however, and are reviewed by Hart.⁵³

Schweitzer and co-workers⁵⁴⁻⁵⁶ have recently challenged the critical state model, suggesting that surface contributions to hysteresis and critical currents are more significant than bulk effects. This was true in some of their samples, which were low- n superconductors with little bulk pinning. Hysteresis only appeared to be surface-controlled in others, in which bulk pinning was so great that internal flux gradients were very steep, and the Bean penetration depth remained small compared with specimen dimensions until fields near H_{c2} .^{46,47} Several other results they incorrectly used to reject the critical state model can easily be interpreted in terms of it.

The existence of surface contributions to hysteresis and critical currents in the mixed state had been noted earlier,⁵⁷ and has since been well documented by many workers. This requires, however, not rejection of the critical state model, but incorporation into it. These effects can be treated by modifying the surface boundary conditions

* Although most experiments deal with the case of field transverse to the transport current, the critical state model has also been successful in the more complicated case of longitudinal field.³⁷

applied to the critical state model, and can be experimentally separated from bulk effects by varying specimen size or with certain ac measurements.⁵⁸ For inhomogeneous high-field (high κ) superconductors of ordinary dimensions, however, most experiments indicate that bulk currents are much more important than surface currents. Why this is true is noted below under the discussion of surface pinning.

In summary, macroscopic electrical and magnetic properties of high-field superconductors are explainable on the Bean critical state model, and depend on the parameter $J_c(B)$. This parameter in turn depends on the bulk pinning forces on flux threads produced by structural defects. We therefore turn to detailed consideration of flux pinning by various types of defects.

Flux Pinning

We will consider first the basic element of flux pinning, the interaction between a single defect and a single flux thread. The line energy of an isolated flux thread has several components. Each flux thread contains a quasi-normal core roughly a coherence length in radius, which contributes a condensation core energy of roughly $H_c^2 \xi^2/8$ per unit length. The surrounding supercurrent vortex, extending to distances of roughly a penetration depth, λ , contributes a vortex energy mostly produced by the kinetic energy of the supercurrents. For $\kappa \gg 1$, the vortex energy of an isolated flux thread is large compared with the core energy, and therefore roughly equals the total line energy, $\phi_{Hc1}/4\pi$.⁵⁹ However, because the vortex extends over a much larger distance than the core, the maximum possible energy gradients (forces) related to the core and vortex may be comparable.³³ Furthermore, vortex forces will decrease as flux density increases and neighboring vortices overlap, whereas core forces may remain relatively unchanged until near H_{c2} , when cores begin to overlap.

Before making crude calculations of possible pinning forces, we must consider the various types of defects that may serve as pinning centers. Flux pinning by various pinning centers has been reviewed by Dew-Hughes.⁶⁰

Classification of pinning centers. A great variety of microstructural features can interact with flux threads. It is convenient³³ to classify them according to the number of dimensions of the pinning entity that are large compared with d , the flux thread spacing. Note that a given element of microstructure may change classification as B increases, since d decreases as $(\phi_0/B)^{1/2}$ (For $B = 20$ Oe, $d = 1 \mu$; for $B = 2000$ Oe, $d = 1000$ A; for $B = 200\ 000$ Oe, $d = 100$ A.)

- A. Zero: "Point" pins - The major classes here are voids, second-phase particles, and defect clusters (such as produced by radiation damage).
- B. One: "Line" pins - The major defect in this category is the dislocation. However, several metallurgical processes can produce rod-like second-phase particles, and some radiation damage tracks may have this dimensionality.
- C. Two: "Surface" pins - This category includes stacking faults, grain and subgrain boundaries, twin and transformation boundaries, and inter-phase boundaries. For completeness, we can also include the external surface of the specimen as a special case of surface pinning.
- D. Three: "Volume" pins - Large voids or particles could easily be larger than d in all dimensions.

"Point" pins. Critical currents in NbTi alloys are enhanced by a dispersion of fine precipitates produced by heat treatment.⁶¹ A commercially-available Nb₃Sn material is believed to derive its current-carrying capacity, at least in part, from an intentionally-introduced dispersion of fine ZrO₂ particles.⁶² Thus point pins are of

practical as well as fundamental interest. We will find, however, that most clear-cut structure-properties experiments have been done on "model" type II superconductors, rather than on practical high-field superconductors.

We will first consider the significance of the nature of the pinning center, and will later consider the importance of the size and spacing of the pins.

A variety of second-phase particles can be used for pinning centers. The particle can itself be a superconducting metal, a normal metal, a semiconducting material, or a nonconducting material. A void can be considered as an extreme example of the last case. Another special case of interest is a paramagnetic or ferromagnetic particle.

Theoretical considerations and several experimental results suggest that the greater is the difference between the superconducting or electronic properties of the particle and those of the matrix, the greater will be the pinning force. That is, a normal particle will provide stronger pinning than a superconducting particle, and an oxide particle or void would provide still stronger pinning.

The distinction between normal and superconducting pins is supported by the observations of Levy et al.⁶³ on eutectic alloys, but was most clearly demonstrated in an experiment on PbInSn alloys.⁶⁴ Here the tin-rich pinning centers were superconducting, but had a lower critical temperature and critical field than the PbIn matrix. Thus as temperature or field was increased, the particles become normal. Critical currents were found to increase with increasing field and temperature, in contrast to usual behavior, proving that normal particles pin more strongly than superconducting particles. [This result also provides an approach to control the temperature and field dependence of critical currents. This may be significant in controlling magnetic instabilities (flux jumps), in which dJ_c/dT plays an important role.⁵³]

Returning to voids, we can make a rough calculation of the pinning forces involved. Consider a spherical void of diameter $D \approx \xi$. The condensation energy of the core will completely disappear where it intersects the void, producing a decrease in energy of $(H_c^2 \xi^2/8) \times D$ over a distance D of flux thread motion, yielding a pinning force of roughly $H_c^2 \xi^2/8$. If $H_c = 3000$ Oe and $\xi = 100$ Å, the force is roughly 10^{-6} dyn. If the flux thread intersects one such void each 1000 Å along its length, $f_p = 10^{-1}$ dyn/cm, and $J_c = 5 \times 10^6$ A/cm². Larger voids can produce larger forces per void by also decreasing much of the vortex energy,^{45,47,48} but intervoid spacing would necessarily be larger, and achievable critical current densities would be of the same order of magnitude.

The calculated interaction force between a ferromagnetic particle and flux thread⁵¹ is comparable to that produced by a void, but the weakening of superconductivity in the surrounding matrix produced by large magnetic fields and a strong proximity effect probably greatly weakens the net effect on J_c . The major interesting feature of ferromagnetic pinning centers is the ability to change the pinning force from attractive to repulsive by varying the direction of magnetization. Because attractive forces produce a higher J_c , ferromagnetic pins can produce critical currents dependent on the sense of the applied magnetic field.⁵¹

Turning now to the optimum size for pinning centers, it is generally agreed that pinning decreases for pinning centers smaller than a coherence length, ξ , and for centers bigger than the interthread spacing, d . Since d approaches ξ near H_{c2} , it follows that optimum pinning center size is roughly a coherence length. There is some experimental verification of this concept. The decrease in J_c with the coarsening of pinning centers larger than a coherence length has been observed in several systems.^{33,57,65} Where pinning centers are smaller than a coherence length, coarsening should increase J_c , and this has been observed in an AlZn alloy.⁶⁶ The quantitative interpretation of these results, however, is complicated by the fact that both size and spacing of pinning

centers change during coarsening, and more careful experiments are necessary to separate these effects.

Considering spacing separately, it seems obvious that J_c will increase with increasing density N of pins per unit volume. If one assumes that every pin produces a force f , then $J_c = 10 Nf/B$. However, several factors will work against this linear increase with N . First, as an increasing volume fraction of the sample becomes occupied by pinning centers, let us say voids, the amount of superconducting matrix available to carry supercurrent of course decreases. Thus, there will eventually be a maximum in J_c with increasing volume fraction of voids.⁶⁷

Second, as the density of pins increases, it becomes increasingly difficult for the flux threads to utilize all the available pinning forces. For example, if the intervaid spacing is less than d , a flux thread may be able to move so that some voids are pinning its core, but others will be distributed throughout the vortex, producing weaker forces directed in various directions. Furthermore, strong interthread forces make it impossible to deflect each flux thread independent of its neighbors. Anderson and Kim³⁰ reasoned that these interthread forces were large to distances of the order of λ , so that a flux-thread lattice would remain virtually undistorted over a "flux bundle" of this size.* One quantitative approach to account for this effect is to assume that the net pinning experienced by the flux bundle will be proportional to the statistical imbalance of forward and reverse pinning forces over the flux bundle volume.^{51,70} This will lead to a J_c proportional not to the pinning center density N , but to \sqrt{N} . (This statistical weakening of the net pinning force would be less significant if pinning centers had a regular spacing that matched the flux-thread spacing. The match, however, would occur only at one sharply-defined flux density. Furthermore, such structural regularity is very unlikely, except for artificially-produced structures, or structures produced by spinoidal decomposition⁷¹ or two-phase directional solidification.⁷²)

There is a clear-cut need for better data on the effect of pinning center density and distribution on J_c . Radiation damage is perhaps the most promising way of achieving such data, although there is some uncertainty as to the nature of the radiation damage centers themselves. Several experimenters have demonstrated an increase in J_c with increasing radiation damage. Such work is reviewed by Cullen.⁷³

"Line" pins. The major new feature here is the possibility of anisotropic properties if the rod-like pins are all parallel. If the pins produce attractive forces, as would voids, maximum pinning would be expected with the field directed parallel to the rods. If the forces were repulsive, optimum forces may be expected with fields normal to the rods. Under certain assumptions,³⁶ the geometric nature of this transverse case can lead to J_c proportional to $B^{-\frac{1}{2}}$, a behavior approximately observed in some materials.

The major line defect in materials, of course, is the dislocation. The effects of dislocations on superconducting properties have been reviewed by van Gorp and van Ooijen.⁷⁴ Experiments on many superconducting alloys show that the production of dislocations during cold work can greatly increase J_c . Calculation of the elastic dislocation-flux thread interaction has been attempted by several authors.⁷⁵⁻⁷⁸ It is here found convenient to consider the effect of a flux thread on the line energy of a dislocation, rather than vice versa. The flux thread core is viewed as a normal filament with slightly different interatomic distances and elastic modulus than the superconducting matrix. These calculations yield a force of about 10^{-8} dyn for a single dislocation-flux thread intersection.

* Although early experiments by Träuble and Essmann⁶⁸ appeared to observe flux bundles directly, these observations are now believed to be artifacts.⁶⁹

Whereas these elastic effects can be related to the effect of the dislocation's stress field on H_c , another possible interaction is through the effect of a locally decreased mean free path on κ . This has not yet been rigorously calculated, but the resulting force may be significantly greater.⁷⁴ An even larger effect might be expected if the dislocation were "decorated" by impurity segregation which further decreased the local mean free path. The pinning force still, of course, will be much less than would be produced by a rod-like void.

After remarking that "none of these treatments comes even close to a satisfactory solution" to the problem of the interaction between the dislocation microstructure and the flux lattice, Seeger and Kronmüller⁷⁹ have recently set up complex "micromagnetic" equations to treat this problem. We must await further work, however, to see if these equations can produce useful results.

Experimental determination of the dislocation-flux thread pinning force has been attempted,⁸⁰⁻⁸² but several complications in the interpretation of the data remain, including the question of flux lattice rigidity and statistical cancellation of forces discussed earlier. A recent paper⁸² concludes that the elementary dislocation-flux thread interaction force is roughly 10^{-7} dyn.

Several experimental results^{83,84} suggest that a given number of dislocations produces a higher J_c when clustered into sub-boundaries than when isolated. Dislocations in cold-worked metals often form structures of low-dislocation-density cells separated by high-dislocation-density cell walls. (Because precipitates can play a significant role in controlling this cell structure, they may have both a direct and indirect effect on flux pinning.) It has been suggested^{74,83,84} that the decreased mean free path in the cell walls, and the corresponding increase in κ , is the major source of the pinning forces. In our classification, of course, these cell walls, or dislocation sub-boundaries, are "surface" pins between two regions of different κ .⁶⁰

"Surface" pins. Again, anisotropy is expected. Optimum J_c is expected when both field and current are parallel to the pinning surface, i.e., when the "Lorentz force" is normal to it. Anisotropy has been demonstrated for external surfaces,⁸⁵ grain boundaries,⁸⁴ and martensitic transformation boundaries.⁸⁶ In samples where most of the internal boundaries are parallel to each other and not perfectly perpendicular to the Lorentz force, flux travels across the sample by moving parallel to the boundaries rather than intersecting them. This "guided flux motion" produces controllable transverse voltages.⁸⁷

An alteration in flux thread density near grain boundaries in thin foils has been directly observed by Essmann and Träuble.²³ These workers have not yet studied type II superconductors carrying transport current. However, they have studied the effect of transport current on thin foils of type I superconductors, in which the intermediate state consists of a flux lattice of multi-quantum flux tubes.⁸⁸ Current induces motion of the tubes, and the interference of grain boundaries and slip planes with flux motion is directly observed.

Campbell et al.³³ have found that J_c in various PbBi alloy samples was proportional to the total interphase surface area. They also found that a given amount of internal surface carried the same current as the same amount of external surface. Since most metallurgical two-phase microstructures have much more internal than external surface, this demonstrates that bulk currents will usually far exceed surface currents.

Campbell et al. also present a detailed model of surface pinning that predicts $J_c(B)$ proportional to $M_r(B)/B^{1/2}$, where $M_r(B)$ is the reversible magnetization expected for a homogeneous sample. This was the dependence observed experimentally. A discrepancy in the constant of proportionality, however, suggests that surface roughness may be significant. Other workers have suggested that pinning of transverse flux at

surface irregularities may control the magnitude of surface currents.⁸⁵

Levy et al.⁶³ have also demonstrated a proportionality between J_c and interphase surface area in a variety of eutectic alloys. Kramer and Rhodes⁸⁹ correlated J_c and internal surface area, but did not find simple proportionality.

Several workers have observed a dependence of J_c on grain size^{90,91} and related this to pinning by grain boundaries. Although this is a possible interpretation, it also should be noted that the procedures that were used to produce samples of different grain size were also likely to produce different dislocation densities within the grains, which may have been the major source of variations in J_c . Witcomb et al.⁹² report that both grain boundaries and mechanical twin boundaries are relatively ineffective at pinning flux in MoRe alloys.

Surface pinning should be greatest when the surface lies between the superconductor and a void or nonconducting particle. Such a surface also produces a sheath of enhanced superconductivity. Extremely high J_c would be obtained in a multiple-layer sample of alternating superconductor and oxide, where the sample approaches an assembly of thin films.

"Volume" pins. It was pointed out by Campbell et al.³³ that although the line energy of a flux thread would be lowered anywhere within a large void or normal precipitate, the changes in energy, or pinning forces, are only associated with entry and exit of the flux thread, i.e., its surfaces. Thus "volume" pins are really "surface" pins, and therefore become less effective as they coarsen.

Flux pinning was originally discussed^{29,30} in terms of the pinning of "flux bundles" by volume pins, and a similar model has recently been employed by Maxwell et al.⁹³ to explain a striking "peak effect" in NbN.

Flux lattice effects. Although we have discussed primarily the interaction forces between a single flux thread and a single defect, we have noted that the strong interaction between flux threads can play a major role in influencing the net pinning forces per unit volume, hence J_c , particularly when the distance between pinning centers becomes less than λ . In a recent paper, Träuble and Essmann²⁵ purport to show that the individual defect-flux thread interaction force is two orders of magnitude greater than the average net force inferred from the flux gradient. Although the validity of their calculation of the individual pinning force is in doubt, a substantial reduction in net effect probably generally occurs because of a statistical cancellation of individual pinning forces. This is expected to be true particularly when the density of pinning centers is high.

The real physical case, the interaction between defects and a flux lattice, is a very complicated problem. Several approaches to the problem have been attempted (Refs. 51,70,94-96). One interesting approach⁶⁹ is to focus attention on the flux-lattice dislocations (FLD's) (Figs. 2 and 3). We have noted the relation between FLD's and flux gradients. It has also been suggested⁹⁷ that flux motion down flux gradients may be accomplished by FLD motion. This suggests that defect pinning of FLD's may be an appropriate model for flux pinning. This approach has not yet been fully evaluated.

Our major hope for improved understanding of this complex problem probably lies with experiments that directly observe the flux lattice, how it is altered in the presence of specific defects, and how it moves under applied currents. Only preliminary observations of defect-flux interactions have been made to date with the Träuble-Essmann fine-powder technique.^{23,88,98} Additional experiments will certainly be forthcoming. More suitable for studying dynamic effects, however, would be the Faraday technique. This technique has recently been greatly improved in resolution,⁹⁹ and may eventually be able to resolve individual flux threads in motion.

Thermal stability. In actual use of high-field superconductors in high-field magnets, it has been found that thermal instabilities (flux jumps) make it impossible to use the full current-carrying capability of the superconductor. Large amounts of normal metal must be included for stability, and this greatly decreases the over-all current density of the windings. In considering flux pinning, therefore, it is significant to ask how the basic nature of the pinning centers may influence thermal instabilities. It seems likely that pinning centers designed from this point of view, even though they may not yield maximum pinning forces or maximum J_c in a short-sample test, may give a material with higher usable J_c in magnet applications.

One factor already mentioned is the ability to control dJ_c/dT using weakly superconducting pinning centers.⁶⁴ High-specific-heat centers would also contribute to stability. Also helpful might be high-conductivity pinning centers, that increase magnetic time constants and decrease thermal time constants. Finally, improved uniformity of pinning center distribution would be very desirable. None of these approaches has yet been evaluated in practical materials.

IV. SUMMARY

Critical temperatures and critical fields of high-field superconductors are less influenced by metallurgical structure than are critical currents. However, for high-field superconducting compounds, particularly of the β -tungsten structure, there is need for more study of the effect of order, stoichiometry, and alloying on critical temperatures and fields.

Critical currents are controlled by interaction between the metallurgical microstructure of the sample and the magnetic microstructure (flux thread lattice) of the mixed state. The balance between flux pinning forces and flux gradient forces (Lorentz forces) determines J_c . A great variety of metallurgical defects have been shown to produce flux pinning.

Consideration of "point" pinning centers suggests that voids or nonconducting particles roughly a coherence length in size may provide optimum pinning forces. Critical currents will no longer increase appreciably with increasing pinning center density when the spacing between centers becomes less than a penetration depth. More experiments with carefully-controlled pinning centers are necessary to test these conclusions.

Although there is ample experimental and theoretical evidence that dislocations can provide flux pinning, it remains in doubt whether the basic interaction is primarily an elastic or a mean free path effect. Several experiments suggest that dislocations are most effective when clustered into sub-boundaries.

Rod-like or lamellar pinning centers may have certain advantages, but properties will depend sensitively on field orientation. If pinning centers are large, only their surfaces contribute to pinning forces, leading to critical currents proportional to internal surface area. External surfaces can also carry current, but bulk currents usually dominate.

A major problem in quantitative understanding of flux pinning is to relate single defect-flux thread pinning forces to the net pinning force exerted on the flux lattice as a whole. Direct-observation experiments are expected to throw light on this problem.

In considering the most desirable pinning centers, it may not be best to optimize net pinning forces and J_c . Because thermal instabilities play such a major role in limiting the applications of high-field superconductors, more thought should be given to the effect of the nature and distribution of pinning centers on thermal instabilities.

REFERENCES

1. J.D. Livingston and H.W. Schadler, *Prog. Mater. Sci.* 12, 183 (1964).
2. H. Bell, Y.M. Shy, D.E. Anderson, and L.E. Toth, *J. Appl. Phys.* 39, 2797 (1968).
3. B.W. Roberts, in Progress in Cryogenics (Academic Press, New York, 1964), Vol. 4, p. 159.
4. N. Pessall and J.K. Hulm, *Physics* 2, 311 (1966).
5. B.T. Matthias, T.H. Geballe, L.D. Longinotti, E. Corenzwit, G.W. Hull, R.H. Willens, and J.P. Maita, *Science* 156, 645 (1967).
6. S. Foner, E.J. McNiff, Jr., B.T. Matthias, and E. Corenzwit, in Proc. 11th Intern. Conf. Low Temperature Physics, St. Andrews, 1968.
7. T.H. Geballe, B.T. Matthias, J.P. Remeika, A.M. Clogston, V.B. Compton, J.P. Maita, and H.J. Williams, *Physics* 2, 293 (1966).
8. T.R. Finlayson, E.R. Vance, and W.A. Rachinger, *Phys. Letters* 26A, 474 (1968).
9. G.D. Cody, these Proceedings, p. 405.
10. T.G. Berlincourt and R.R. Hake, *Phys. Rev.* 131, 140 (1963).
11. L.E. Toth, C.M. Yen, L.G. Rosner, and D.E. Anderson, *J. Phys. Chem. Solids* 27, 1815 (1966).
12. C.M. Yen, L.E. Toth, Y.M. Shy, D.E. Anderson, and L.G. Rosner, *J. Appl. Phys.* 38, 2268 (1967).
13. L.E. Toth, Report on Air Force Grant AFOSR 1012-66 (1967).
14. B.B. Goodman, *Phys. Letters* 1, 215 (1962).
15. G.D. Cody, J.L. Cooper, and G.W. Cullen, U.S. Air Force Technical Report AFML-TR-65-169, p. 96 (1965).
16. R.R. Hake, *Appl. Phys. Letters* 10, 189 (1967).
17. I.S. Jacobs and J.D. Livingston, unpublished results (1967).
18. R.G. Boyd, *Phys. Rev.* 153, 444 (1967).
19. D.R. Tilley, *J. Phys. C (Proc. Phys. Soc.)* 1, 293 (1968).
20. D. Cribier, B. Jacrot, B. Farnoux, and L. Madhav Rao, *J. Appl. Phys.* 37, 952 (1966).
21. W. Fite, II, and A.G. Redfield, *Phys. Rev. Letters* 17, 381 (1966).
22. U. Essmann and H. Träuble, *Phys. Letters* 24A, 526 (1967).
23. U. Essmann and H. Träuble, *Phys. Letters* 27A, 156 (1968).
24. H. Träuble and U. Essmann, *Phys. Stat. Sol.* 25, 373 (1968).
25. H. Träuble and U. Essmann, *J. Appl. Phys.* 39, 4052 (1968).
26. R. Labusch, *Phys. Letters* 22, 9 (1966).
27. C.P. Bean, *Phys. Rev. Letters* 8, 250 (1962); *Rev. Mod. Phys.* 36, 31 (1964).
28. H. London, *Phys. Letters* 6, 162 (1963).
29. P.W. Anderson, *Phys. Rev. Letters* 9, 309 (1962).
30. P.W. Anderson and Y.B. Kim, *Rev. Mod. Phys.* 36, 39 (1964).
31. Y.B. Kim, C.F. Hemstead, and A.R. Strnad, *Phys. Rev.* 129, 528 (1963).
32. W.A. Fietz, M.R. Beasley, J. Silcox, and W.W. Webb, *Phys. Rev.* 136, A335 (1964).
33. A.M. Campbell, J.E. Evetts, and D. Dew-Hughes, *Phil. Mag.* 18, 313 (1968).

34. W.F. Druyvesteyn, Phys. Letters 14, 275 (1965).
35. M.A.R. LeBlanc, Phys. Rev. Letters 11, 149 (1963).
36. K. Yasukochi, T. Ogasawara, N. Usui, and S. Ushio, J. Phys. Soc. Japan 19, 1649 (1964); J. Phys. Soc. Japan 21, 89 (1966).
37. B.C. Belanger, Ph.D. Thesis U.S.C. (1968); Bull. Am. Phys. Soc. 13, 361 (1968); to be published.
38. J.E. Evetts, D. Dew-Hughes, and A.M. Campbell, Phys. Letters 16, 113 (1965).
39. P.S. Swartz, Phys. Rev. Letters 9, 448 (1962).
40. J.J. Hauser, Phys. Rev. Letters 9, 423 (1962).
41. T.W. Grasmehr and L.A. Finzi, IEEE Trans. on Magnetics MAG-2, 334 (1966).
42. C.P. Bean, R.L. Fleischer, P.S. Swartz, and H.R. Hart, Jr., J. Appl. Phys. 37, 2218 (1966).
43. H.R. Hart, Jr., and P.S. Swartz, U.S. Air Force Technical Report AFML-TR-65-431 (1966).
44. Reviewed by S.L. Wipf, these Proceedings, p. 511.
45. H.T. Coffey, Cryogenics 7, 73 (1967).
46. H.E. Cline, R.M. Rose, and J. Wulff, J. Appl. Phys. 37, 1 (1966).
47. J. Friedel, P.G. deGennes, and J. Matricon, Appl. Phys. Letters 2, 119 (1963).
48. J. Silcox and R.W. Rollins, Appl. Phys. Letters 2, 231 (1963).
49. F. Irie and K. Yamafuji, J. Phys. Soc. Japan 23, 255 (1967).
50. S.H. Goedemoed, P.H. Kes, F. Th. A. Jacobs, and D. deKlerk, Physica 35, 273 (1967).
51. T.H. Alden and J.D. Livingston, J. Appl. Phys. 37, 3551 (1966).
52. H.T. Coffey, Phys. Rev. 166, 447 (1968).
53. H.R. Hart, Jr., these Proceedings, p. 571.
54. D.G. Schweitzer and B. Bertman, Phys. Letters 20, 339 (1966).
55. D.G. Schweitzer, M. Garber, and B. Bertman, Phys. Rev. 159, 296 (1967).
56. D.G. Schweitzer and M. Garber, Phys. Rev. 160, 348 (1967).
57. J.D. Livingston, Rev. Mod. Phys. 36, 54 (1964).
58. H.A. Ullmaier, Phys. Stat. Sol. 17, 631 (1966).
59. A.A. Abrikosov, J. Phys. Chem. Solids 2, 199 (1957).
60. D. Dew-Hughes, Mater. Sci. Eng. 1, 2 (1966).
61. D. Kramer and C.G. Rhodes, Trans. AIME 236, 1612 (1967).
62. M.G. Benz, Trans. AIME 242, 1067 (1968).
63. S.A. Levy, Y.B. Kim, and R.W. Kraft, J. Appl. Phys. 37, 3659 (1966).
64. J.D. Livingston, Appl. Phys. Letters 8, 319 (1966).
65. J.D. Livingston, J. Appl. Phys. 34, 3028 (1963).
66. G.A. Beske, P. Hilsch, and J. Wulff, Trans. AIME 239, 890 (1967).
67. J.A. Catterall and I. Williams, J. Less-Common Metals 12, 258 (1967).
68. H. Träuble and U. Essmann, Phys. Stat. Sol. 20, 95 (1967).
69. H. Träuble, private communication.

70. J.I. Gittleman and B. Rosenblum, J. Appl. Phys. 39, 2617 (1968).
71. J.W. Cahn, Trans. AIME 242, 166 (1968).
72. G.A. Chadwick, Prog. Mater. Sci. 2, 2 (1963).
73. G.W. Cullen, these Proceedings, p. 437.
74. G.J. van Gorp and D.J. van Ooijen, J. Physique 27, C3-51 (1966).
75. R.L. Fleischer, Phys. Letters 3, 111 (1962).
76. W.W. Webb, Phys. Rev. Letters 11, 191 (1963).
77. E.J. Kramer and Ch. L. Bauer, Phil. Mag. 15, 1189 (1967).
78. K. Yamafuji, F. Irie, and C.L. Bauer, Phys. Rev. Letters 20, 658 (1968).
79. A. Seeger and H. Kronmuller, Phys. Stat. Sol. 27, 371 (1968).
80. E. Nembach, Phys. Stat. Sol. 13, 543 (1966).
81. E. Nembach, H. Freyhardt, and P. Haasen, Phys. Stat. Sol. 18, 807 (1966).
82. H. Freyhardt and P. Haasen, Z. Metallk. 58, 856 (1967).
83. A.V. Narlikar and D. Dew-Hughes, J. Mater. Sci. 1, 317 (1966).
84. G.J. van Gorp, Philips Res. Repts. 22, 10 (1967).
85. P.S. Swartz and H.R. Hart, Jr., Phys. Rev. 137, A818 (1965); Phys. Rev. 156, 412 (1967).
86. G.J. van Gorp, Phys. Stat. Sol. 17, K135 (1966).
87. A.K. Niessen, J. van Suchtelen, F.A. Staas, and W.F. Druyvesteyn, Philips Res. Repts. 20, 226 (1965).
88. H. Träuble and U. Essmann, Phys. Stat. Sol. 25, 395 (1968).
89. D. Kramer and C.G. Rhodes, J. Inst. Metals 94, 261 (1966).
90. J.J. Hanak and R.E. Enstrom, in Proc. Tenth Intern. Conf. Low Temperature Physics, Moscow, 1966, Vol. 2B, p. 10.
91. K.J. Gifkins, C. Malseed, and W.A. Rachinger, Scripta Met. 2, 141 (1968):
92. M.J. Witcomb, A. Echarri, A.V. Narlikar, and D. Dew-Hughes, J. Mat. Sci. 3, 191 (1968).
93. E. Maxwell, B.B. Schwartz, H. Wizgall, and K. Hechler, J. Appl. Phys. 39, 2568 (1968).
94. K. Yamafuji and F. Irie, Phys. Letters 25A, 387 (1967).
95. R. Labusch, to be published.
96. W.W. Webb, these Proceedings, p. 396.
97. F.C. Frank, unpublished (1963).
98. N.V. Sarma, Phil. Mag. 17, 1233 (1968).
99. H. Kirchner, Phys. Letters 26A, 651 (1968).

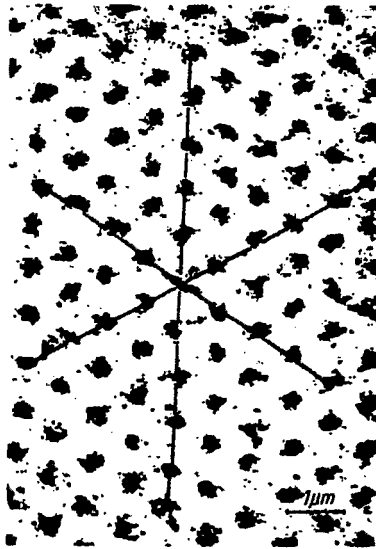


Fig. 1. Flux thread lattice in Pb-6.33 at.% In at 1.2°K. Remanent state, $B = 70$ Oe. Flux threads are made visible by deposition of fine ferromagnetic particles. (After Träuble and Essmann, Ref. 24.)

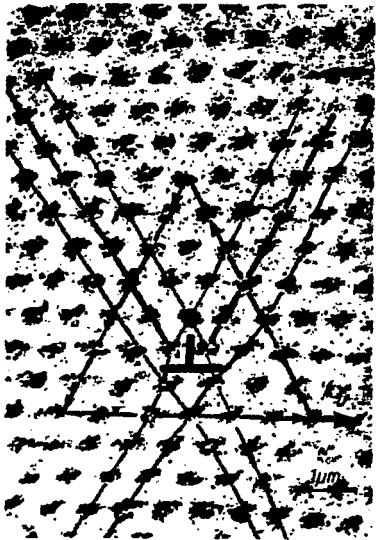


Fig. 2. Edge dislocation in the flux thread lattice. (After Träuble and Essmann, Ref. 24.)

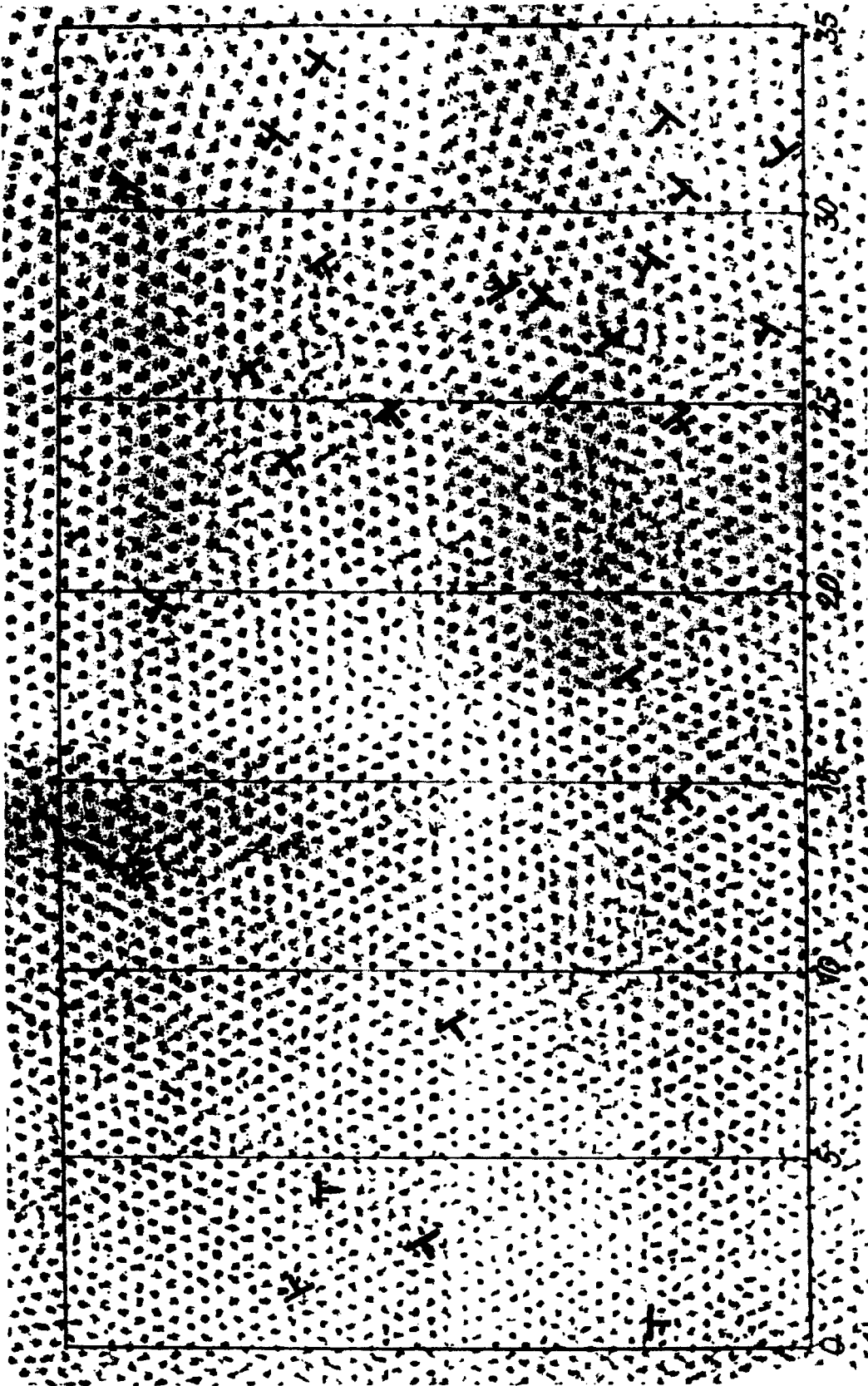


Fig. 3. Flux lattice with flux density gradient from right to left. Dislocation cores are indicated by the symbol X. (After Träuble and Essmann, Ref. 25.)

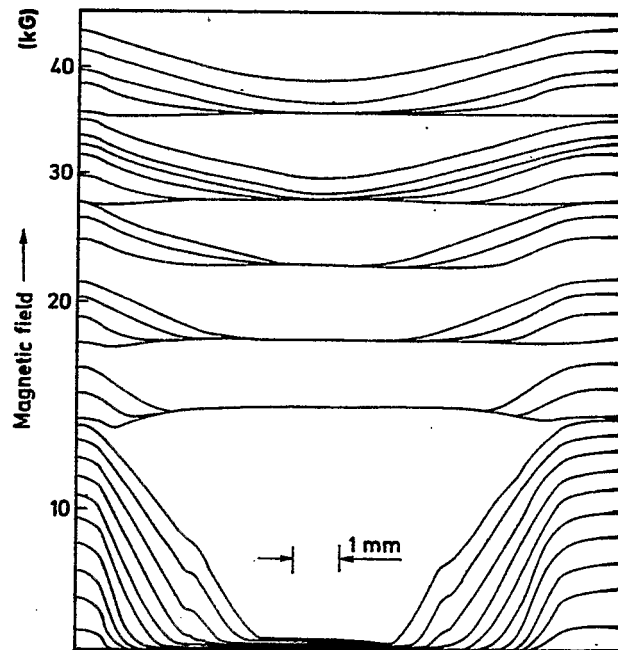


Fig. 4. Field distribution in a NbTi sample in increasing field, as measured by driving a Hall probe through a fine transverse gap in the sample. (After Coffey, Ref. 45.)